



Research Article

D. Kaya and K. Kececi / Hacettepe J. Biol. & Chem., 2019 47 (1), 67–76

Hacettepe Journal of Biology and Chemistryjournal homepage: www.hjbc.hacettepe.edu.tr

Effect of Surface Functionalization on the Transport Characteristics of Methyl Orange Through Track-Etched Membranes

Yüzey Fonksiyonlandırmanın Metil Oranjın İz-Aşındırılmış Membranlardan Taşınım Özelliklerine Etkisi

Dila Kaya[✉] and Kaan Kececi^{✉*}

Department of Chemistry, Istanbul Medeniyet University, Istanbul, Turkey.

ABSTRACT

In this study we have prepared cylindrical and conical nanopores on poly(ethylene terephthalate) (PET) membranes using track-etching method. Later on we have investigated the mass transport of the chosen model dye Methyl Orange (MO) through these membranes. In order to enhance the transport flux of the dye, we have used surface functionalization using ethylenediamine (EDA) as the functionalization agent. We have confirmed the functionalization of the nanopore surface using electrochemical measurements. We have investigated mass transport through functionalized and bare PET membranes and shown that by attaching amine groups on the nanopore walls, we can indeed increase the transport of MO. Effects of pore size, pore geometry and temperature were investigated for the transport of MO. We have shown that PET, which has a negative surface charge at neutral pH, can be functionalized for a more effective transport of negatively charged analyte.

Keywords

Track-etched nanopore; mass transport; PET membrane; surface functionalization.

Öz

Bu çalışmada, iz-aşındırma yöntemiyle poli(etilen tereftalat) (PET) membranlar üzerinde silindirik ve konik nanogözenekler hazırlanmıştır. Daha sonra seçilen model boyalı metil oranjin (MO) bu membranlardan kütle taşınması araştırılmıştır. Boyanın akışını artırmak için, fonksiyonlandırma aracı olarak etilen diamin (EDA) kullanarak nanogözenek yüzeyi modifiye edilmiştir. Elektrokimyasal ölçümler sayesinde nanogözenek yüzeyinin kaplandığı doğrulanmıştır. Fonksiyonel hale getirilmiş ve boş PET membranlardan kütle taşınımı araştırılmış ve nanogözenek duvarlarına amin grupları ekleyerek, MO taşınımının gerçekten artırılabileceği gösterilmiştir. MO'nun taşınımına gözenek büyülüğu, gözenek geometrisi ve sıcaklığın etkileri araştırılmıştır. Nötral pH'ta negatif yüzey yüküne sahip olan PET'nin, negatif yüklü analitin daha etkin bir şekilde taşınması için fonksiyonlandırılarak işlevsel hale getirebileceği gösterilmiştir.

Anahtar Kelimeler

İz-aşındırılmış nanogözenek; kütle taşınımı; PET membran; yüzey fonksiyonlandırma.

Article History: Received: Aug 08, 2018; Revised: Jan 08, 2019; Accepted: Jan 14, 2019; Available Online: Mar 01, 2019.**DOI:** 10.15671/HJBC.2019.276**Correspondence to:** K. Kececi T, Department of Chemistry, 34700, İstanbul Medeniyet University, İstanbul, Turkey.**E-Mail:** kaan.kececi@medeniyet.edu.tr

INTRODUCTION

In the last few years, nanopores formed in a variety of solid materials have found important use in several areas including sensing [1-4], separation [5,6] and even single molecule analysis [7]. Depending on the chosen fabrication method, multipores or single nanopores can be prepared. The nanoporous structures can be biological or synthetic. However, there are many shortcomings of biological nanopores which limit their use such as their fragility, instability under some pH and temperature values and their size. Therefore, the chemically and mechanically robust synthetic nanopores which can be low cost, user-friendly and sensitive are highly on demand [8]. Other advantages of synthetic nanopores over their biological counterparts include the ability to control the pore geometry, easy functionalization of the pore surface and possibility of integration with electronic or optical systems [9-11].

A number of techniques have been proposed for the preparation of synthetic nanopores [12-15]; while each of them have their certain advantages, track-etching method stands out as it allows precise control over nanopore geometry and size, enables tailoring of the surface properties and is economically feasible. In track-etching, polymer membranes are irradiated with heavy ion(s) (i.e. Au) and during this process these ions leave tracks along their routes. By chemically etching these sensitive tracks, they turn into nanopores [16]. If the membrane had been irradiated with a single heavy ion, a single nanopore is obtained which is mostly used for the determination and sensing at a molecular level. Multiple nanopores formed by the etching of tracks created by multiple heavy ions (i.e. 10^8 ions) are mostly implemented in studies for the selective transport or separation of molecules. By modifying the etching process, pores with different geometries and sizes can also be obtained.

Multipores can be fabricated on a variety of materials such as silicon [17], silicon nitride [18,19], graphene [20] and anodic alumina oxide [21,22]. One of the most frequently used materials is anodic alumina oxide, but the thickness of these membranes are not suitable as the molecular flow is very low. Furthermore the techniques for forming nanopores on silicon and silicon nitride are very expensive as they require special equipment. Since the desired attributes for solid-state nanopores are that they are highly durable, robust, reproducible, allow high molecular flux and also economical; nanopores obtained by track-etching on polymer membranes can be preferred

for effective separation and transport applications [23]. Some widely used polymers for track-etching include polycarbonate (PC), poly(ethylene terephthalate) (PET) and polyimide (PI).

Functionalization of the nanopore surface is also possible for enhanced, selective transport and sensing. Besides having adjustable pore geometry and size; track-etched polymer membranes are also preferred for allowing easy surface modification [23]. During the track-etching process, chemical groups are generated on pore surfaces which are prone to functionalization with a variety of groups such as macromolecules [5,24,25], amphoteric chains [26], amines [27], boronic acid [28] etc. Another approach for modifying the surface is first covering the nanopore walls with gold using electroless plating method and then attaching certain groups via thiol chemistry [29-31]. The purpose of functionalization ranges from changing the surface charge, to implementing a pH or temperature responsive group and modifying the surface with agents that allow the binding of only specific groups.

Nanoporous membranes with desired pore size, density and thickness are alternatives for controlled release of pharmacological agents [32], drug delivery systems [33] and also for biomedical applications [34]. Lately, processes in which membranes are used for protein separation have also gained importance in biotechnology [35]. Especially, the discrimination and separation between molecules based on their surface charge, size or hydrophobicity using nanopores hold promise for future studies. But before these membranes can be used in such technologies, some aspects of the fabrication and the transport need to be explored and clarified. Firstly, the fabrication of reproducible nanopores with the appropriate geometry and size need to be established. Then the selectivity of the nanopore towards the analyte needs to be enhanced by functionalization or the optimization of the transport properties. So it can be said that there is still room for improvement on analyte transport from nanoporous membranes and further studies are necessary.

In this work, we have prepared nanopores on PET membranes using symmetrical and asymmetrical track-etching method for obtaining cylindrical and conical membranes, respectively. The surface of PET membranes is known to possess negative carboxyl ($-COO^-$) groups at neutral pH due to track-etching process. Taking advantage of these negatively charged groups, we have functionalized the nanopore surface with ethylenediamine (EDA) using

EDC chemistry. We have confirmed the functionalization using electrochemical measurements. Finally, we have investigated the transport properties of the azo dye methyl orange through bare and functionalized PET membranes under varying conditions of pore size, temperature and pore geometry, and shown that surface modification enhances the flux of the negatively charged analyte.

MATERIALS and METHODS

Poly (ethylene terephthalate) (PET) membranes (3 cm diameter, 12 μm thickness) were obtained from Gesellschaft für Schwerionenforschung (GSI, Darmstadt-Germany) commercially. The membranes have been irradiated with heavy ions (i.e., Au ion, 11.4 MeV) at different ion densities ranging from 1 to 10^9 ions/membrane. All the membranes were exposed to UV irradiation (254 nm) prior to chemical etching in order to saturate the damages in tracks, resulting in homogeneous size distribution. All solutions were prepared from deionized water (Millipore Direct-Q 5, Millipore Co.). Formic acid (HCOOH), sodium hydroxide (NaOH), methyl orange ($\text{C}_{14}\text{H}_{14}\text{N}_3\text{NaO}_3\text{S}$) (Figure 1) and potassium chloride (KCl) were purchased from Sigma Aldrich and used as received without further purification. 1-Ethyl-3-(3-dimethylaminopropyl) carbodiimide hydrochloride (EDC, Thermo Scientific), N-hydroxysulfosuccinimide (Sulfo-NHS, Thermo Scientific), ethylenediamine dihydrochloride (EDA, Aldrich) and 2-(N-morpholino) ethanesulfonic acid (MES, Alfa Aesar), were used as received for the chemical functionalization.

Fabrication of Nanopores

Purchased tracked PET membranes (single and multi-tracked) were irradiated with long-wave UV irradiation overnight to sensitize the tracks and enable a more homogeneous size distribution. Cylindrical nanopores were obtained on PET membranes using symmetrical

track- etch method. Shortly, batch etching was performed and track membranes were suspended in a beaker filled with the etching solution (9 M NaOH) at room temperature. Afterward, the membrane was kept in a beaker filled with stopping solution (1 M HCOOH) for 30 minutes to stop the etching process. Finally, the membrane was washed with di-water to remove residues from the membrane surface.

For obtaining conically shaped nanopores a previously discussed asymmetric chemical etching technique was used [36]. With this purpose, the membrane was mounted between the two halves of a conductivity cell with one side of the membrane facing the etching solution (9 M NaOH) and the other side facing the stopping solution (1 M HCOOH and 1 M KCl). Platinum (Pt) electrodes were immersed into each cell and 1 V transmembrane potential was applied to monitor the breakthrough moment where a sharp increase is observed in the current (Keithley 6487 picoammeter/voltage source, Cleveland, OH, USA). After the etching process, the etching solution was replaced with stopping solution for neutralization. Then, both cells were rinsed with di-water to remove possible residues from the membrane surface. In the end, conically shaped nanopore was obtained with two different sized openings called base (large opening) and tip (small opening). The large opening of the nanopore (d_{base}) was directly determined from SEM images of multipore membranes while electrochemical measurements were performed for the calculation of small opening (d_{tip}) of the conical membrane. With this purpose, both halves of the conductivity cell were filled with electrolyte solution (i.e., 1 M KCl, 10 mM PBS buffer at pH = 7) while the single nanopore membrane was mounted between these cells. Ag/AgCl electrodes were used and potential was stepped between -1 V and +1 V. The resistance of the nanopore (R) is proportional to the conductivity of solution (σ) the length of nanopore (l , thickness of the membrane), d_{base}

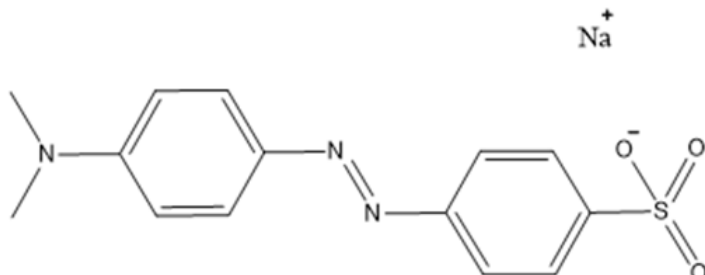


Figure 1. Methyl orange (azo dye, M: 327.33 g/mol).

and d_{tip} as given in Equation 1. R-value was the reciprocal of the slope of I-V curve obtained from the electrochemical measurement and the tip diameter was calculated using Equation 1. (Conductivity measurements were carried out with a Mettler Toledo FE 30 conductivity meter.)

$$R = \frac{4\rho l}{\pi d_{tip} d_{base}} \quad (1)$$

Functionalization of the Nanopore Surface

It was discussed in the introduction that carboxylate groups are generated on the PET nanopore walls due to the track-etching procedure. The well-established EDC chemistry was used for functionalizing the pore surface with ethylenediamine (EDA) through amide bond formation. Firstly, the membrane was immersed in a solution prepared in 10 mM MES buffer ($\text{pH} = 4.6$) that contains 1 mM EDC and 1 mM S-NHS. EDC reacts with the carboxyl group on the membrane surface to form an amine-reactive intermediate. Sulfo N-hydroxysuccinimide (S-NHS) must be present in the medium for stabilization of the intermediate. After 1 hour, the membrane was taken out of this solution and immersed in 1 mg/ml EDA dissolved in di-water overnight. The reaction intermediate interacts with EDA added to the amide to form the amide bond. Finally,

the membrane was rinsed several times with distilled water to remove salts from the surface. The schematic representation of the process is given in Figure 2. Functionalization of the surface was confirmed by current-voltage measurements of single nanopore membranes.

Current-Voltage Measurements

In order to confirm that the pore surface was indeed modified with EDA, current-voltage (I-V) characteristics were taken into account. For these measurements, bare and EDA-modified single conical nanopore membrane was mounted between the two halves of the conductivity cell. Both halves of the cell were filled with 0.1 M KCl solution in PBS buffer at pH 7 as the electrolyte solution. An Ag/AgCl electrode was inserted into each half-cell, and a picoammeter/voltage source (Keithley 6487, Keithley Instruments, Cleveland, OH, USA) was used to apply transmembrane potential and measure the ionic current across the membrane. The potential was stepped 50 mV between -1 V and +1 V, and I-V curves were obtained. In the case of conical nanochannels, anode was placed at the side of the membrane with the big opening of the channel.

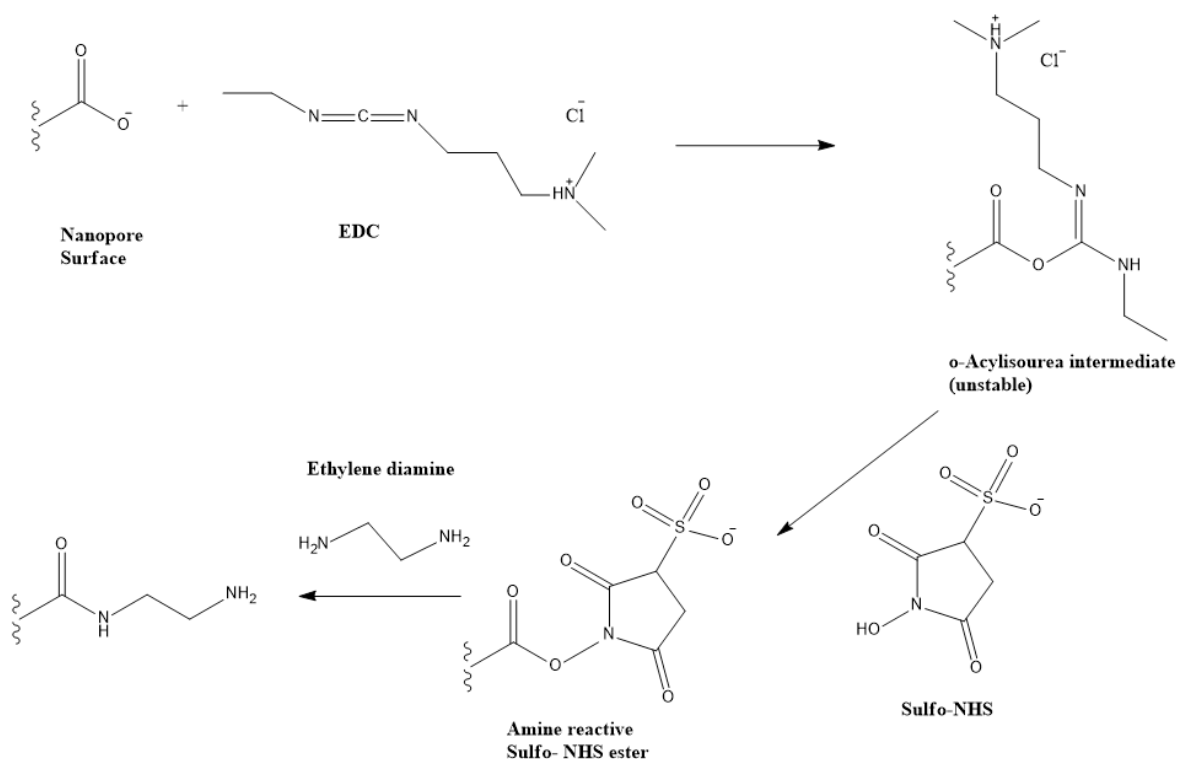


Figure 2. Functionalization steps of the nanopore surface with EDC chemistry.

Mass Transport Experiments

The membranes were placed in an H-cell to investigate the transport properties of MO. The cell volumes were 5 mL with an effective permeation area of 0.35 cm². The known concentration of the analyte (2 mM) in phosphate buffer (10 mM, pH = 7) was placed in the feed half-cell and the permeate half-cell contained only pure buffer solution. Phosphate buffer at pH 7 was selected because at neutral pH, nanopore surface charge of PET membrane is negative due to the –COO⁻ groups on its pore walls [37] and also at this pH, methyl orange is negatively charged ($pK_a = 3.47$). Throughout the experiment, both half cells were continuously stirred with a magnetic stirrer (~1050 rpm). Samples were collected from the permeate side at regular time intervals and the concentration of the analyte was determined using a UV-Vis spectrophotometer (Shimadzu-2600) and the linear calibration curve of MO of known concentrations.

RESULTS and DISCUSSION

Determination of Etching Rate

Pore diameters of cylindrical pores and base diameters of the conical nanopores were obtained directly from the SEM images of multipore membranes (10⁹ nanopores/cm²). An average of 20 pores were used to calculate the diameters using Image-J software, and standard deviation values were taken into account. SEM images (at 8000 magnification) of multipore PET membranes symmetrically etched for different

times are shown in Figure 3. A linear relationship was established between pore size and etching time. The bulk etching rate, which was obtained from the slope of the obtained linear plot (not shown), was found to be $4.45 \pm 0.3 \text{ nm} \cdot \text{min}^{-1}$. Nanopores with desired sizes were produced by etching the required time accordingly with this etching rate.

Confirmation of the Surface Functionalization

In order to confirm that the PET nanopore surface was indeed modified with EDA, I-V curves of bare and modified membranes were obtained. Asymmetric nanopores in PET are known to cause a phenomena called ion current rectification (ICR). ICR can be described as a non-linear behavior in the ionic current even though the electrolyte concentration on both sides of the pore are the same [38]. ICR can be calculated as the ratio of current values at -1 V and +1 V. Since PET nanopores have a negative surface charge at neutral pH due to the carboxylate groups produced during chemical etching; at neutral pH, the ICR is expected to be higher than 1. But if the surface charge is removed the I-V curve would become more linear. So it can be said that the I-V curves and ICR provide information about the surface charge of PET nanopores [29]. Figure 4 shows the I-V curves of the bare and modified PET membrane.

It can be seen in Figure 4 that prior to modification PET shows a non-linear current-voltage curve, which is in agreement with literature. After modification with EDA,

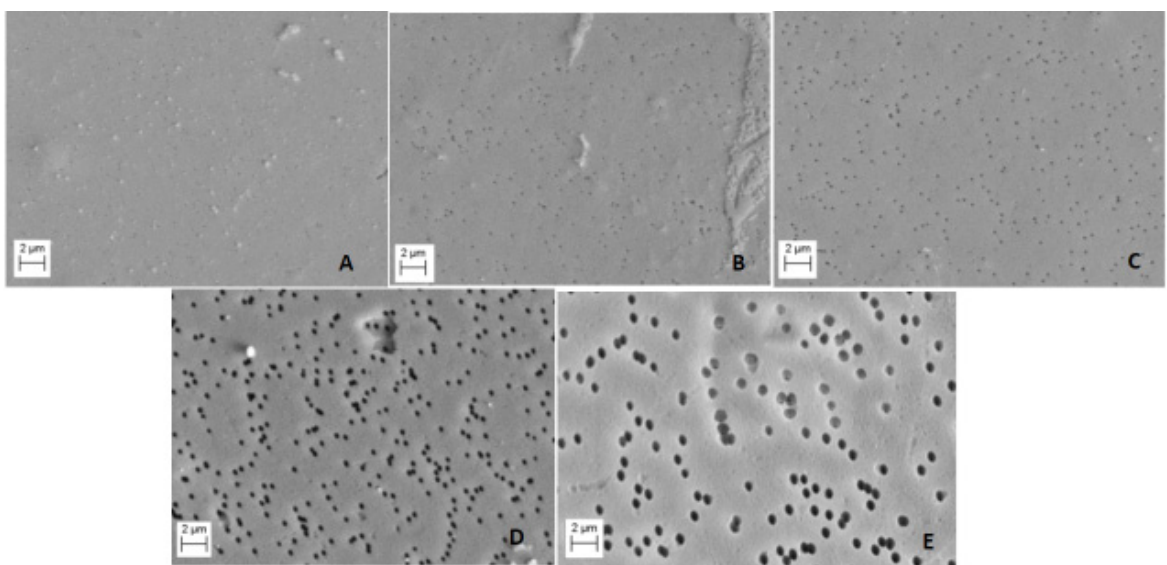


Figure 3. SEM images of multiporous PET etched for A) 30 mins, B) 45 mins, C) 60 mins, D) 90 mins, E) 120 mins.

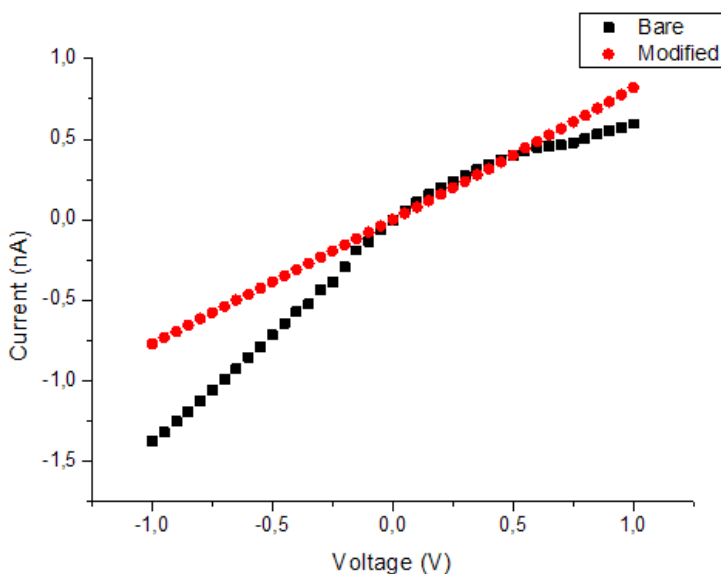


Figure 4. Current-voltage curves of bare and modified PET in 0.1 M KCl (pH = 7).

I-V curve becomes entirely linear which indicates that the membrane has indeed gone through the functionalization and no longer has negative groups on its pore walls.

Another important result of the obtained I-V curves is that when the tip diameters of bare and modified PET membranes were calculated, they were found to be 17.3 nm and 15.7 nm, respectively. This result indicates that the change in diameter of the pore after functionalization is negligible especially for pores with larger sizes.

Mass Transport of MO Through Bare and Modified PET Membranes

For the mass transport experiments of MO, a multiporous (10^9 pore. cm^{-2}) PET membrane with 50 ± 4 nm cylindrical nanopores was used. The transport of the dye was conducted using bare and EDA functionalized membranes and continued for three hours. Figure 5 shows the linear relationship between molecular flux (transported amount of the analyte per cm^2) and time with R^2 values of 0.989 and 0.990 for bare and modified

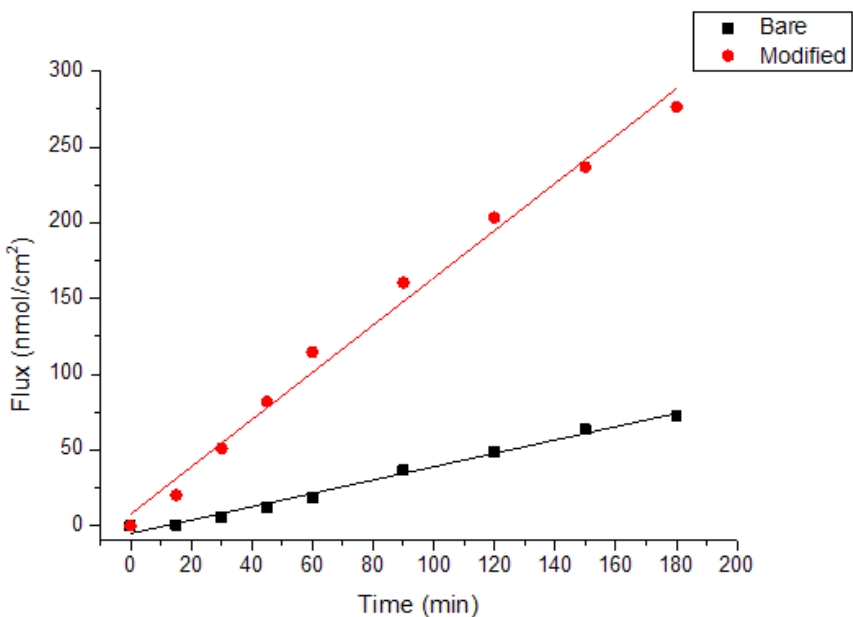


Figure 5. Flux of MO through 50 ± 4 nm nanopores (Pore density: 10^9 pore/ cm^2).

nano pores, respectively. The transport rate was calculated from the slope of the obtained line, which yielded the amount of analyte transferred per unit time.

Transport rates of MO through bare and modified PET were calculated to be 0.44 and $1.56 \text{ nmol.cm}^{-2}.\text{min}^{-1}$ respectively. This finding indicates that after the surface functionalization, the molecular flux increased almost 3.5 times while still increasing linearly with time.

Effect of Pore Size on Transport Rate

In order to investigate the dependency of molecular transport to nanopore size, cylindrical nanopores with different diameters were prepared and used for the transport of MO. The molecular flux values of MO through 50 ± 4 , 100 ± 11 and 150 ± 17 nm bare and modified nanopores after three hours are given in Figure 6. As it was previously discussed, we have neglected the change in diameter of the pore after functionalization. Because I-V results indicated that this change was very small and negligible.

The transport is only due to diffusion from feed cell to the permeate cell because of the concentration gradient since there is no electric field applied and therefore no

transmembrane potential. So as the nanopore diameter was increased from 50 to 150 nm, the diffusion of the MO molecules became easier and this was represented as an increase in the flux. Functionalization of the nanopore surface also enhanced the transport from nanopores of all sizes. The transport rates for bare and modified nanopores with various diameters are presented in Table 1. According to Table 1, the highest enhancement of the transport rate after functionalization was obtained with 100 ± 11 nm nanopores.

Effect of Temperature on Transport Rate

Effect of temperature on the transport rate was also investigated. With this purpose, the transport of MO through cylindrical 100 ± 11 nm pore membrane was performed at four different temperature values. The same membrane was then modified with EDA, and MO transport at the same temperature values was investigated. The obtained transport rate values are given in Table. 2.

According to the obtained results, the transport rate increased from 1.61 to $7.26 \text{ nmol.cm}^{-2}.\text{min}^{-1}$ when the temperature was raised from 293 K to 323 K , respectively. This positive dependence of diffusion coefficient to

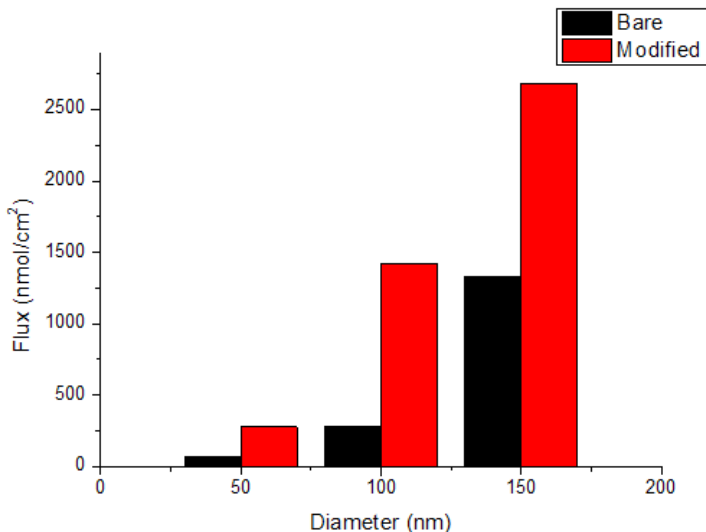


Figure 6. Flux of MO through pores with different diameters.

Table 1. Transport rates of bare and modified nanopores with various diameters.

| Diameter (nm) | Rate ($\text{nmol.cm}^{-2}.\text{min}^{-1}$) | | Enhancement (x times) |
|---------------|--|----------|--------------------------|
| | Bare | Modified | |
| 50 ± 4 | 0.44 | 1.56 | 3.5 |
| 100 ± 11 | 1.60 | 7.49 | 4.7 |
| 150 ± 17 | 7.27 | 13.95 | 1.9 |

Table 2. Transport rates of bare and modified nanopores at various temperatures.

| Temperature (K) | Rate (nmol.cm ⁻² .min ⁻¹) | | Enhancement (x times) |
|-----------------|--|----------|-----------------------|
| | Bare | Modified | |
| 293 | 1.61 | 7.48 | 4.65 |
| 303 | 1.89 | 8.02 | 4.24 |
| 313 | 2.52 | 9.90 | 3.92 |
| 323 | 7.26 | 28.22 | 3.88 |

temperature indicated that the transport mechanism was endothermic and favored higher temperatures. Arrhenius equation can be used to explain the temperature dependence of diffusion coefficient (Equation 2); where D is the diffusion coefficient, D_0 is the diffusion coefficient at infinite temperature, E_a is the activation energy, T is the absolute temperature, and k is the Boltzmann constant.

$$D = D_0 e^{-\frac{E_a}{kT}} \quad (2)$$

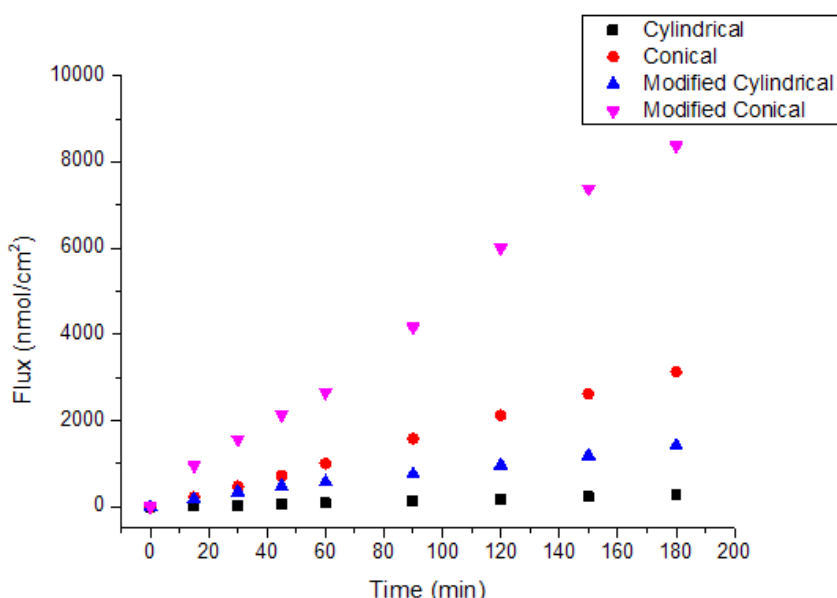
Mass transport of MO through modified nanopores was also faster than bare nanopores (Table 2). Also similar to the bare ones, transport from modified nanopores favored higher temperatures and an increase in transport rate was 3 to 4 times higher than the bare ones.

Effect of Pore Geometry on Transport Rate

To investigate the effect of pore geometry on the transport rate of MO, PET membranes with conical pores were fabricated using asymmetric etching method. The obtained bare conical membranes were used for the mass transport of MO and afterward functionalized with EDA using EDC chemistry. The prepared modified nanopores were also used for mass transport experiments.

In order to be able to compare cylindrical and conical nanopores, the conical pores were also fabricated to have tip openings of 100 nm. With this purpose a second etching step was carried out [39]. With the first etching step, nanopores with base diameters of 232 nm and tip diameters of 17 nm were fabricated. Then, after the first step, a more dilute etching solution (2 M NaOH) used for etching this time and a transmembrane potential (1 V) was applied. The current was monitored, and when it reached a certain value the etching process was stopped and stopping solution (1 M HCOOH + 1 M KCl) was introduced to both half cells. Once more, the half cells were rinsed with water to remove residues. The tip diameter of the obtained conical nanopore was 100 nm. The etching process was initially used to fabricate single nanopores for an easier application of the protocol, and the same procedure was carried out for the fabrication and second step etching of multipores.

The membrane was placed in the H-cell with the tip side of the membrane facing the feed cell and the transport of MO through the conical nanopores was performed. The dependence of MO flux to nanopore geometry for bare and modified nanopores is given in Figure 7. It can be said that according to flux values conical geometry is

**Figure 7.** Flux of MO through pores with different geometries (bare and modified).

certainly more efficient than cylindrical geometry for mass transport of MO. After functionalization, transport from both cylindrical and conical nanopores became faster, but this increase was more significant for the conical geometry.

Overall, it was shown that the conical geometry which forms a trapping zone at the tip entrance enhances the transport of the analyte and increases the transport rate. This promotive effect was expected as it was previously reported by us [40] and others [41]. But in this work, we have also shown that this promotive effect can be enhanced four times by modifying the surface.

Conclusion

In this work, we have prepared cylindrical and conical nanopores on PET membranes and demonstrated the effect of nanopore surface functionalization on the mass transport of MO dye. Using electrochemical measurements and I-V characteristics, we have confirmed the functionalization of the nanopore surface. We have also shown the effects of pore size, pore geometry and temperature on the transport rate. As the pore size increased, it was found that the transport rate increased as well. This was attributed to the easier diffusion of dye molecules through the membrane. Temperature was also found to increase the transport rate for both bare and modified nanoporous membranes. When symmetrical and asymmetrical geometries were taken into account, it was shown that due to the trapping zones formed near the entrance of the pore, transport through conical nanopores were much faster. This positive effect on transport rate was even further enhanced after surface functionalization. With this work we have shown that nanoporous membranes prepared by the track-etching method can be used for mass transport applications. Since the control over pore size and geometry is possible and the surface can be functionalized accordingly to the analyte, development of selective membranes with desired properties is possible and should be studied further.

References

1. Q. Zhai, J. Wang, H. Jiang, Q. Wei, E. Wang, Bare conical nanopore embedded in polymer membrane for Cr(III) sensing, *Talanta*, 140 (2015) 219-225.
2. Y.R. Kim, J. Min, I.H. Lee, S. Kim, A.G. Kim, K. Kim, K. Namkoong, C. Ko, Nanopore sensor for fast label-free detection of short double-stranded DNAs, *Biosens. Bioelectron.*, 22 (2007) 2926-2931.
3. B.M. Venkatesan, A.B. Shah, J.M. Zuo, R. Bashir, DNA Sensing Using Nanocrystalline Surface-Enhanced Al₂O₃ Nanopore Sensors, *Adv. Funct. Mater.*, 20 (2010) 1266-1275.
4. L.T. Sexton, P. Jin, K. Kececi, L. Baker, Y. Choi, C.R. Martin, Resistive pulse sensing of proteins using single conical nanopores in PET membranes, *Abstr. Pap. Am. Chem. S.*, 231 (2006).
5. E.N. Savariar, K. Krishnamoorthy, S. Thayumanavan, Molecular discrimination inside polymer nanotubules, *Nat. Nanotechnol.*, 3 (2008) 112-117.
6. A.S. Prabhu, T.Z.N. Jubery, K.J. Freedman, R. Mulero, P. Dutta, M.J. Kim, Chemically modified solid-state nanopores for high throughput nanoparticle separation, *J. Phys. Condens. Matter*, 22 (2010) 454107.
7. B. Hornblower, A. Coombs, R.D. Whitaker, A. Kolomeisky, S.J. Picone, A. Meller, M. Akeson, Single-molecule analysis of DNA-protein complexes using nanopores, *Nat. Meth.*, 4 (2007) 319.
8. C. Dekker, Solid-state nanopores, *Nat. Nanotechnol.*, 2 (2007) 209-215.
9. R. Patricio, A. Pavel Yu, C. Javier, M. Salvador, Pore structure and function of synthetic nanopores with fixed charges: tip shape and rectification properties, *Nanotechnology*, 19 (2008) 315707.
10. D. Kaya, A. Dinler, N. San, K. Kececi, Effect of Pore Geometry on Resistive-Pulse Sensing of DNA Using Track-Etched PET Nanopore Membrane, *Electrochim. Acta*, 202 (2016) 157-165.
11. B.A. Sartowska, O.L. Orelovitch, A. Presz, P.Y. Apel, I.V. Blonskaya, Nanopores with controlled profiles in track-etched membranes, *Nukleonika*, 57 (2012) 575-579.
12. O.A. Saleh, L.L. Saw, Biological sensing with an on-chip resistive pulse analyzer, *P. Ann. Int. IEEE Embs*, Vols 1-7, 26 (2004) 2568-2570.
13. H.M. Kim, M.H. Lee, K.B. Kim, Theoretical and experimental study of nanopore drilling by a focused electron beam in transmission electron microscopy, *Nanotechnology*, 22 (2011) 275303.
14. T. Deng, M. Li, Y. Wang, Z. Liu, Development of solid-state nanopore fabrication technologies, *Chin. Sci. Bull.*, 60 (2015) 304-319.
15. K. Healy, B. Schiedt, A.P. Morrison, Solid-state nanopore technologies for nanopore-based DNA analysis, *Nanomedicine (Lond)*, 2 (2007) 875-897.
16. D. Kaya, K. Kececi, Preparation of nanopores and their application for the detection of metals, *Bulg. Chem. Commun.*, 49 (2017) 37-42.
17. S.R. Park, H. Peng, X.S. Ling, Fabrication of nanopores in silicon chips using feedback chemical etching, *Small*, 3 (2007) 116-119.
18. I. Vlassiouk, P.Y. Apel, S.N. Dmitriev, K. Healy, Z.S. Siwy, Versatile ultrathin nanoporous silicon nitride membranes, *Proc. Natl. Acad. Sci. USA*, 106 (2009) 21039-21044.
19. K. Briggs, H. Kwok, V. Tabard-Cossa, Automated fabrication of 2-nm solid-state nanopores for nucleic acid analysis, *Small*, 10 (2014) 2077-2086.

20. S. Garaj, W. Hubbard, A. Reina, J. Kong, D. Branton, J.A. Golovchenko, Graphene as a subnanometer trans-electrode membrane, *Nature*, 467 (2010) 190-U173.
21. M. Lillo, D. Lasic, Ion-beam pore opening of porous anodic alumina: The formation of single nanopore and nanopore arrays, *Mater. Lett.*, 63 (2009) 457-460.
22. S. Kipke, G. Schmid, Nanoporous alumina membranes as diffusion controlling systems, *Adv. Funct. Mater.*, 14 (2004) 1184-1188.
23. R. Spohr, Status of ion track technology-prospects of single tracks, *Radiat. Meas.*, 40 (2005) 191-202.
24. S. Nasir, M. Ali, W. Ensinger, Thermally controlled permeation of ionic molecules through synthetic nanopores functionalized with amine-terminated polymer brushes, *Nanotechnology*, 23 (2012) 225502.
25. B. Yameen, M. Ali, R. Neumann, W. Ensinger, W. Knoll, O. Azzaroni, Synthetic Proton-gated ion channels via single solid-state nanochannels modified with responsive polymer brushes, *Nano Lett.*, 9 (2009) 2788-2793.
26. M. Ali, P. Ramirez, S. Mafé, R. Neumann, W. Ensinger, A pH-tunable nanofluidic diode with a broad range of rectifying properties, *ACS Nano*, 3 (2009) 603-608.
27. K. Kececi, L.T. Sexton, F. Buyukserin, C.R. Martin, Resistive-pulse detection of short dsDNAs using a chemically functionalized conical nanopore sensor, *Nanomedicine*, 3 (2008) 787-796.
28. Q.H. Nguyen, M. Ali, R. Neumann, W. Ensinger, Saccharide/glycoprotein recognition inside synthetic ion channels modified with boronic acid, *Sens. Actuat. B*, 162 (2012) 216-222.
29. Z. Siwy, E. Heins, C.C. Harrell, P. Kohli, C.R. Martin, Conical-nanotube ion-current rectifiers: The role of surface charge, *J. Am. Chem. Soc.*, 126 (2004) 10850-10851.
30. C.C. Harrell, P. Kohli, Z. Siwy, C.R. Martin, DNA - Nanotube artificial ion channels, *J. Am. Chem. Soc.*, 126 (2004) 15646-15647.
31. K.B. Jirage, J.C. Hulteen, C.R. Martin, Effect of thiol chemisorption on the transport properties of gold nanotubule membranes, *Anal. Chem.*, 71 (1999) 4913-4918.
32. T.A. Desai, S. Sharma, R.J. Walczak, A. Boiarski, M. Cohen, J. Shapiro, T. West, K. Melnik, C. Cosentino, P.M. Sinha, Nanoporous implants for controlled drug delivery, in *BioMEMS and Biomedical Nanotechnology*, 2006, Springer. p. 263-286.
33. G. Jeon, S.Y. Yang, J.K. Kim, Functional nanoporous membranes for drug delivery, *J. Mater. Chem.*, 22 (2012) 14814-14834.
34. S.P. Adiga, C. Jin, L.A. Curtiss, N.A. Monteiro-Riviere, R.J. Narayan, Nanoporous membranes for medical and biological applications, *Wiley Interdiscip. Rev. Nanomed. Nanobiotechnol.*, 1 (2009) 568-581.
35. A. Saxena, B.P. Tripathi, M. Kumar, V.K. Shahi, Membrane-based techniques for the separation and purification of proteins: an overview, *Adv. Coll. Interf. Sci.*, 145 (2009) 1-22.
36. K. Kececi, N. San, D. Kaya, Nanopore detection of double-stranded DNA using a track-etched polycarbonate membrane, *Talanta*, 144 (2015) 268-274.
37. Z. Siwy, P. Apel, D. Baur, D.D. Dobrev, Y.E. Korchev, R. Neumann, R. Spohr, C. Trautmann, K.O. Voss, Preparation of synthetic nanopores with transport properties analogous to biological channels, *Surf. Sci.*, 532 (2003) 1061-1066.
38. Z.S. Siwy, Ion-Current Rectification in Nanopores and Nanotubes with Broken Symmetry, *Adv. Funct. Mater.*, 16 (2006) 735-746.
39. J.E. Wharton, P. Jin, L.T. Sexton, L.P. Horne, S.A. Sherrill, W.K. Mino, C.R. Martin, A method for reproducibly preparing synthetic nanopores for resistive-pulse biosensors, *Small*, 3 (2007) 1424-1430.
40. D. Kaya, K. Keçeci, Transport Characteristics of Selected Dyes Through Track-Etched Multiporous PET Membranes, *Hacettepe J. Biolog. Chem.*, 46 (2018) 1-11.
41. Q.H. Nguyen, M. Ali, S. Nasir, W. Ensinger, Transport properties of track-etched membranes having variable effective pore-lengths, *Nanotechnology*, 26 (2015) 485502.